Multiscale Simulations of Spray Drying Process

Thi Thu Hang Tran*

Hanoi University of Science and Technology – No. 1, Dai Co Viet Str., Hai Ba Trung, Ha Noi, Viet Nam
Received: December 09, 2017; Accepted: November 26, 2018

Abstract

Spray drying process for powder production is widely commercialized in diary industrial sector. In this paper, a multiscale study of spray drying process with skim milk served as drying product is presented. Firstly, a characteristic drying curve model is developed to describe the heat and mass transfer of single droplet drying process. The parameters of the characteristic drying curve model are established based on the experimental observation. Then, the single droplet drying characters are incorporated into a computational fluid dynamic (CFD) solver to customize the heat, mass and momentum transfer between the droplet/particle and the drying agent flow inside a spray dryer. The CFD simulation results are validated by comparing against the experimental data observed on a pilot-scale spray dryer. A good agreement between numerical and experimental result on both of fluid phase and particle properties indicates the predictability of the CFD simulation. The influence of the drying conditions on the drying efficiency of the tower is also explored in detail.

Keywords: spray drying, CFD simulation, single droplet drying model, characteristic drying curve model, skim milk

1. Introduction

Spray drying is one of the most commonly used drying methods in the production of pharmaceuticals [1], food [2,3] and chemicals [4,5]. Liquid solution or slurry is atomized in a flow of hot drying agent, resulting in fast evaporation of moisture. This drying technique is often recommended for thermally sensitive materials because of the short drying time, which reduces the degradation of drying particles [6,7]. On the one hand, the properties and morphology of the obtained particles are related to the efficiency of the droplet-to-particle transformation process. On the other hand, these particle properties have a large influence on the product quality as well as powder characteristics [8]. To study this relationship is not an easy task, because it is necessary to understand not only the interactions inside individual droplets (micro scale) but also the complex physical phenomena happening in the spray tower (macro scale).

Literature work on spray drying can be classified into experimental and modelling studies. Most experiments were performed in laboratory-scale and pilot-scale spray dryers to investigate the drying of specific materials [9–11]. Unfortunately, the measurement of flow field, air temperature, particle temperature, humidity, particle moisture content, particle size in the large scale is costly and challenging [12,13]. Spray drying modelling is a useful solution for this issue. However, the modelling approach also faces various obstacles such as lacking similarity in the dynamics of small and large spray dryers, the complicated air flow and the different trajectories of particles, the dependence of product quality on particle heating history in the tower, and the difficulty in determining the drying kinetics of droplets/particles during spray drying [14].

For the aforementioned reasons, it is necessary to consider the multi-scale character of spray drying by first investigating single droplet drying and then scaling up to spray drying in the tower. The goal of this work is the development of such multi-scale investigations of spray drying applied to skim milk solutions by accounting for drying kinetics and dried particle morphology of single droplets, as well as spray dryer modelling.

Following this introduction, a characteristic drying curve (CDC) modeling of heat and mass transfer processes during drying process of single droplet is briefly introduced. The parameters of the CDC model are established from the experimental data measured by a droplet suspension system. Next, the CDC model is implemented into a CFD solve, i.e. Ansys Fluent v.13, via user defined functions. The CFD simulation results are tested against the experimental data obtained in a pilot scale spray drying tower. A good agreement between numerical and experimental result on the particle properties indicates the predictability of the CFD simulation. Finally, several conclusions of this work are drawn.

Corresponding author: Tel.: (+84) 961.290.149
Email: hang.tranthithu@hust.edu.vn

2. Single droplet drying model

2.1. Governing equation of CDC model

The drying process is comprised of 2 periods: the constant drying rate (1st) and the falling drying rate (2nd) periods. During the 1st period, the droplet interacts with the drying agent as a pure water droplet and the impact of solid phase on the drying behavior is neglected. The droplet shrinks during this 1st period such that the reduction in its volume is equal to the volume of evaporated water. After that, a dry solid shell forms at the droplet surface and the 2nd period commences. The moisture content at this transition point is denoted as X_{cr}. During the 2nd period, the drying rate is restrained due to the heat and mass transfer resistance of the dry shell. The evaporation rate during the 1st drying period is calculated as

$$\dot{M}_{v,\mathrm{I}} = A\rho_g\beta\left(Y_{sat}\left(T\right)-Y_g\right), \quad (1)$$

where A is the surface area of the droplet/particle, ρ_g is the density of the drying agent and β is the mass transfer coefficient [15]. $Y_{sat}(T)$ and Y_g are the saturated moisture content at the droplet/particle temperature T and the moisture content of the bulk air, respectively. The saturation moisture content is computed as

$$Y_{sat}\left(T\right) = \frac{\tilde{M}_{\mathrm{v}}}{\tilde{M}_a}\frac{p_{v,sat}\left(T\right)}{p_0 - p_{v,sat}\left(T\right)}, \quad (2)$$

where $\tilde{M}_{\mathrm{v}}$ and $\tilde{M}_a$ are the molar mass of vapor and dry air, respectively [15]. $p_{v,sat}(T)$ is the saturation vapor pressure at the droplet/particle temperature T and p_0 denotes the total pressure of the drying agent. The saturation vapor pressure is calculated using the Antoine equation

$$p_{v,sat}\left(T\right) = \exp\left(A - \frac{B}{C+T}\right), \quad (3)$$

where A = 23.196, B = 3816.44 and C = 227.02, and the temperature T is given in ^{o}C [15]. During the 2nd period, the liquid evaporation is restrained due to the appearing of dry shell; therefore the evaporation rate reduces with a factor f which is lower than unity as [15]

$$\dot{M}_{v,\mathrm{II}} = fA\rho_g\beta\left(Y_{sat}\left(T\right)-Y_g\right). \quad (4)$$

Thus, f may be calculated as

$$f = \frac{\dot{M}_{v,\mathrm{II}}}{A\rho_g\beta\left(Y_{sat}\left(T\right)-Y_g\right)} = \frac{\dot{M}_{v,\mathrm{II}}}{\dot{M}_{v,\mathrm{I}}}, \quad (5)$$

which is referred as the retardation coefficient. During both 1st and 2nd drying periods, the evolution of moisture content over time is described by

$$\frac{dX}{dt} = \frac{\dot{M}_v}{M_s}, \quad (6)$$

where M_s is the solid mass of the droplet/particle. The energy conservation equation of the droplet/particle can be written as

$$Mc_p\frac{dT}{dt} = \alpha A\left(T_g - T\right) - \dot{M}_v\Delta h_{evp} \quad (7)$$

$$\text{or } \frac{dT}{dt} = \frac{\alpha A\left(T_g - T\right) - \dot{M}_v\Delta h_{evp}}{Mc_p}, \quad (8)$$

where $M = M_s + M_l$ is the mass of the droplet/particle and c_p is the effective specific heat capacity of the droplet/particle. α denotes the convective heat transfer coefficient, Δh_{evp} is the specific latent heat of evaporation. Conclusively, the governing heat and mass transfer equations of droplet/particle drying process can be written as [15]

$$\frac{dX}{dt} = \frac{fA\rho_g\beta\left(Y_{sat}\left(T\right)-Y_g\right)}{M_s}, \quad (9)$$

$$\frac{dT}{dt} = \frac{\alpha A\left(T_g - T\right) - fA\rho_g\beta\left(Y_{sat}\left(T\right)-Y_g\right)\Delta h_{evp}}{Mc_p}, \quad (10)$$

with $f = 1$ if $X \geq X_{cr}$ and $f < 1$ if $X < X_{cr}$. Practically, the retardation coefficient f can be correlated experimentally as a function of normalized moisture content ϕ defined as [15]

$$\phi = \frac{X - X_{cr,2}}{X_{cr,2} - X_{eq}}, \quad (11)$$

where X_{eq} is the equilibrium moisture content of the particle. In this work, the equilibrium moisture content X_{eq} of skim milk is empirically calculated by using Guggenheim – Anderson – de Boer (GAB) equation [16]. The heat and mass transfer coefficient is calculated by using following correlations

$$Sh = \sqrt{\left(2 + 0.664\,\mathrm{Re}^{1/2}\,Sc^{1/3}\right)^2 + 1.15^2}, \quad (12)$$

$$Nu = \frac{Sh}{Le^{1/3}}, \quad (13)$$

where $Sh = \frac{\beta d}{\delta}$, $Nu = \frac{\alpha d}{\lambda}$, $Re = \frac{v_g d}{\upsilon}$, $Sc = \frac{\upsilon}{\delta}$ and $Le = \frac{Sc}{Pr}$ are the Sherwood, Nusselt, Reynold, Schmidt and Lewis numbers, respectively.

2.2. Parameters of CDC model

To established the parameters of the CDC model, a droplet suspension system shown in Fig. 1 was build up. The most salient feature of this experimental system is that both the changes of droplet/particle mass and droplet/particle diamter can be recorded simultaneously [17]. The solution of skim milk (J.M. Gabler-Saliter, Germany) with different solid mass fractions was employed as drying material. The drying experiments were perfomed with the drying condition presented in Table 1.

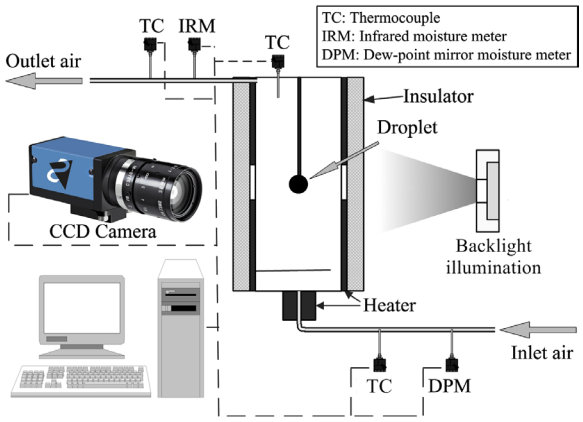

Fig. 1. Suspension droplet drying system.

Table 1. Drying conditions used in single droplet drying experiments.

Parameter	Value
Solid mass fraction, $x_{s,0}$	0.20, 0.30, 0.40, 0.50
Air temperature, T_g	60°C, 100°C, 140°C
Air moisture content, Y_g	4 g/kg
Air velocity, v_g	0.021 m/s

As discussed, the droplet shrinkages during the 1st period, the shrinkage is stop when the 2nd period commences. Therefore, the critical moisture content is determined at the transition point where the droplet diameter does not change further. The calculated critical moisture content is correlated as a following function of drying condition

$$X_{cr} = 0.04354 + \frac{0.24604}{x_{s,0}} + 3.7652\times10^{-5} T_g \,. \qquad (14)$$

The normalized moisture content ϕ and the drying rate retardation coefficient f are calculated based on the drying rate dX/dt and the critical moisture content X_{cr} by using Eqs. 5 and 11, respectively. The calculated drying rate retardation coefficient f is correlated as a power function of the normalized moisture content

$$f = \phi^{a\cdot\phi+b}, \qquad (15)$$

where a and b are the parameters computed as

$$a = -1.434 + 10.856 x_{s,0} - 9.895 x_{s,0}^2 \qquad (16)$$

$$b = 0.602 - 0.92 x_{s,0} + 1.807 x_{s,0}^2 \qquad (17)$$

2.3. Validation of CDC model

In order to assess the accuracy of the developed CDC model, the model predictions are compared to the experimental results obtained. Exemplary comparisons can be are presented in Fig. 2. The CDC model reflects well the drying kinetic curves obtained from the suspension droplet drying experiments. It implies that the proposed parameters (Eqs. 14-17) are reliable and can thus be applied to describe the drying process.

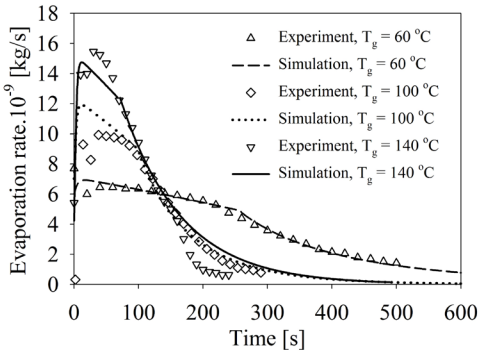

Fig. 2. Comparison of evaporation rates calculated by full SDD and CDC models at different temperature. The experimental data is extracted from [17].

3. CFD simulation

The ANSYS Fluent version 13.0 was employed as CFD solver for simulating the spray drying system on the basis of the Euler-Lagrange approach. In which, the gas phase is treated as continuous phase in steady state by the Reynolds-averaged Navier-Stokes equations combined with the standard k-ε turbulence model. The governing equations are described precisely in the literature and in the ANSYS Fluent theory guide. These equations are therefore not be rewritten here. The simultaneously heat, mass, momentum transport equation are solved iteratively by using the control volume finite element method. The droplets/particles are considered as discrete phase. The CDC model that describes the heat and mass interaction between discrete and continuous phases is implemented into the CFD solver via the user defined function written in C language.

3.1. CFD model configurations

The CFD simulations are performed on a pilot scale spray drying tower (c.f. Fig. 3) with total height of 6100 mm and inner diameter of 400 mm. To avoid heat leak, the tower is issulated externally by 100 mm

glass wool layer, except of a length of 720 mm from the bottom. The ambient air is sucked in by a fan and is heated up by electrical heaters. The hot air enters the drying chamber on top of the tower whereas the exhausted air flow out near the bottom of the tower. The skim milk solution, with initially 30% mass fraction of solid, is atomized on the top of the tower via a thermostated two-fluid nozzle (Schlick, Germany) with narrow spray angle (15-20°). Dried powder is received at the bottom of the drying chamber. The geometry of the pilot-scale tower was discretized to generate the computational mesh which is thereafter imported into the CFD solver. The simulations are performed with several meshes of different mesh density and element shape to obtain accurate solution. Finally, a mesh with 253522 tetrahedral cells, 75271 nodes with minimum orthogonal of 0.28 was chosen to be used in the simulations.

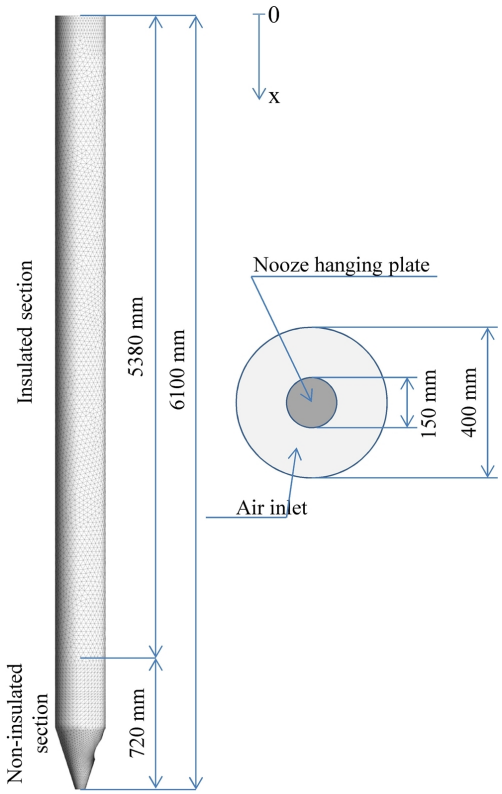

Fig. 3. The computational domain used in CFD simulation.

The following strategy was developed for numerical solutions. First, the flow field of drying air was computed without discrete phase until the converged solution was obtained. Next, spray droplets were injected into the domain and two way coupled calculations were implemented until the converged steady solution was achieved. For the continuous phase, spatial discretization was performed by an upwind scheme of second order for the transport and turbulence model. Pressure was discretized using the PRESTO! scheme. The SIMPLE scheme was used for coupling between the pressure and velocity. Other configurations can be refered to Tran et al. [15].

3.2. CFD simulation results

3.2.1 Simulation validation

To check the model validity, the CFD simulation is performed for feed rate of 172 ml/min and inlet air temperature of 150 ºC. The mas flow rate of inlet air is 0.075 kg/s, whereas the inlet air humidity is 0.006 kg vapor/kg dry air. It takes several hours to accomplished one simulation with a PC with CPU Intel Core i5 and 8 GB RAM. The averaged moisture content of the droplet/particles along vertical direction (from the top towards the bottom of dryer) is compared against the experimental observations in Fig. 4. It can be seen that the CFD simulation results reflect fairly the drying behavior of the tower, with the regression coefficient of R^2 = 0.97. It implies the predictability of the CFD simulation in describing the heat and mass transfer within the considered spray dryer.

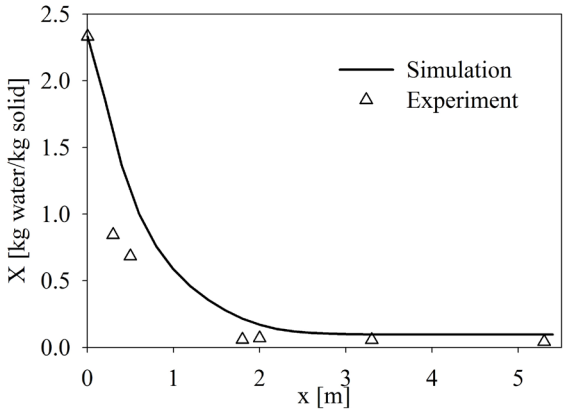

Fig. 4. Numerical and experimental evolutions of averaged moisture content along vertical direction obtained with feed rate of 172 ml/min and inlet air temperature of 150 ºC. The experimental data is extracted from [15].

The temperature, moisture content and velocity fields of the gas phase at the symmetry plane are plotted in Fig. 5. As can be seen, both temperature and moisture content fields vary significantly in the top-half of the tower, in contrast with slightly variations in the bottom-half of the tower. It implies that the drying process mainly occurs in the top-half of the tower which is favored by the evolution of moisture content along the vertical direction (c.f. Fig. 4).

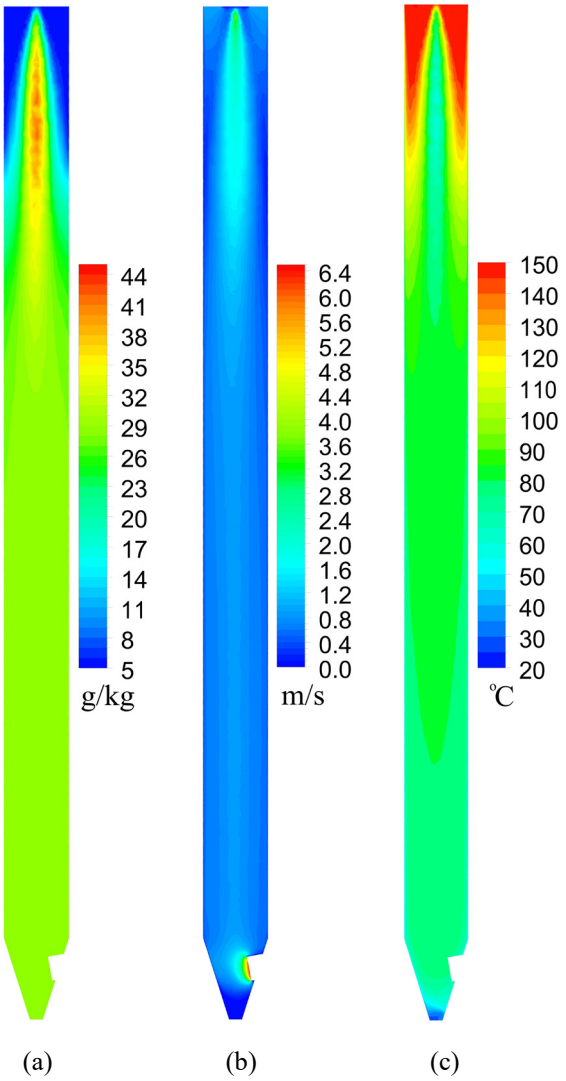

Fig. 5. Moisture content (a), velocity (b) and temperature (c) fields in the symmetry plane obtained with feed rate of 172 ml/min and inlet air temperature of 150 °C, air mass flow rate of 0.075 kg/s.

3.2.2 Sensitivity analysis

In order to optimize the operation of the spray tower, a sensitivity analysis study is performed in this section. Firstly, the influence of inlet air temperature on the drying efficiency is investigated by varying the inlet temperature in between 110 °C and 180 °C whereas other operating conditions of the tower remain unchanged, identical as the simulation case presented in Section 3.2.1. The evolutions of mean moisture content of the droplets/particles along the vertical centerline with different inlet temperature are presented in Fig. 6. As can be seen, the droplets/particles moisture content obtained with $T_{air,inlet}$ = 110 °C still reduces slightly at the bottom of the tower. It implies that the dehydration does not process completely with $T_{air,inlet}$ = 110 °C. With higher inlet air temperature (120 °C, 150 °C, 180 °C, for instance), the moisture content seemingly remains unchanged at the dryer bottom. Conclusively, with the inlet air temperature above 120 °C, the increasing of the inlet air temperature does not enhance significantly the drying process. The reduction of product moisture content with the increasing of drying agent temperature is due to the depending of the milk equilibrium moisture content on the temperature describing via GBA equation.

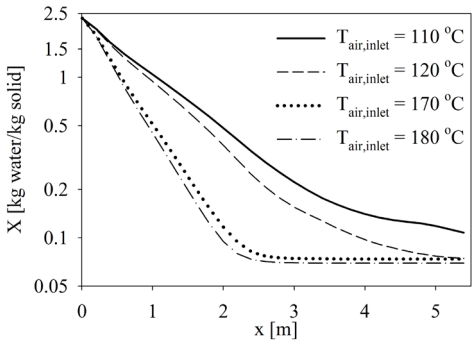

Fig. 6. Influence of inlet air temperature on evolution of droplets/particles moisture content along vertical direction. The feed rate of 172 ml/min and air mass flow rate of 0.075 kg/s remain unchanged for all simulations.

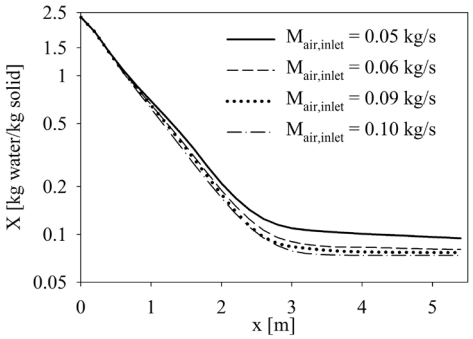

Fig. 7. Influence of inlet air temperature on evolution of droplets/particles moisture content along vertical direction. The feed rate of 172 ml/min and inlet air temperature of 150 °C remain unchanged for all simulations.

Furthermore, the impact of inlet air mass flow rate on the dry efficiency is accessed by varying the mass flow rate of drying agent from 0.05 kg/s to 0.1 kg/s whereas other drying conditions remain unchanged.

With the inlet air mass flow rate of 0.05 kg/s, the product moisture still reduces at the bottom of the tower; whereas with higher mass flow rate (0.06 kg/s, 0.09 kg/s, 0.10 kg/s, for instance) the drying process is almost completed at x ≈ 3.5 m. Thus, with the inlet air mass flow rate higher than 0.06 kg/s, the

increasing of inlet air mass flow rate does not improve the drying efficiency.

4. Conclusion

In this work, a multiscale simulation of skim milk drying process is presented. Based on the experimental results, parameters of a characteristic drying curve model for single skim milk droplet drying are established. This characteristic drying curve model is implemented in a CFD simulation afterward to describe drying process within a spray tower. The CFD simulation results are validated against the experimental observation. On the basic of this validated CFD model, the influences of the inlet air moisture content mass flow rate and temperature on the drying process are explored. The results indicate a possibility in reducing the drying agent temperature and/or flow rate to minimize the energy consumption with the current operating condition and setup.

Several assumptions were made during CFD model developing such as the collision between droplets/particles, the collapse of droplet/particles are neglected. Additionally, the radiation heat transfer between the hot wall surface and droplets/particles is assumed to be negligible. In the future, the further studies shall be carried out to relax these assumption. Under certain circumstances, this proposed multiscale simulation may be applied to optimize the operation of industrial spray tower systems.

Acknowledgments

This research is funded by the Hanoi University of Science and Technology (Project T2017-PC-062).

References

[1] M. Ameri, Y.-F. Maa, Spray drying of biopharmaceuticals: Stability and process considerations, Drying Technology 24 (2006) 763–768.

[2] E.H.-J. Kim, X.D. Chen, D. Pearce, Surface composition of industrial spray-dried milk powders. 1. Development of surface composition during manufacture, Journal of Food Engineering 94 (2009) 163–168.

[3] A. Gharsallaoui, G. Roudaut, O. Chambin, A. Voilley, R. Saurel, Applications of spray-drying in microencapsulation of food ingredients: An overview, Food Research International 40 (2007) 1107–1121.

[4] C.-Y. Su, H.-Z. Tang, K. Chu, C.-K. Lin, Cosmetic properties of TiO2/mica-BN composite powder prepared by spray drying, Ceramics International 40 (2014) 6903–6911.

[5] M. Nakamura, K. Kazuo, T. Arai, S. Toyoda, Multi-stage spray drying method in manufacturing heavy duty detergents, Drying Technology 4 (1986) 67–88.

[6] K. Master, Handbook of spray drying, 3rd ed., George Godwin, London, 1979.

[7] A.S. Mujumdar, Handbook of Industrial Drying, 4th ed., CRC Press Inc, [s.l.], 2014.

[8] E. Tsotsas, Multiscale approaches to processes that combine drying with particle formation, Drying Technology 33 (2015) 1859–1871.

[9] A.M. Goula, K.G. Adamopoulos, Spray drying of tomato pulp: Effect of feed concentration, Drying Technology 22 (2004) 2309–2330.

[10] X. Li, N. Anton, C. Arpagaus, F. Belleteix, T.F. Vandamme, Nanoparticles by spray drying using innovative new technology: the Büchi nano spray dryer B-90, Journal of controlled release official journal of the Controlled Release Society 147 (2010) 304–310.

[11] L. Alamilla-Beltrán, J.J. Chanona-Pérez, A.R. Jiménez-Aparicio, G.F. Gutiérrez-López, Description of morphological changes of particles along spray drying, Journal of Food Engineering 67 (2005) 179–184.

[12] C. Anandharamakrishnan, Computational fluid dynamics applications in food processing, Springer New York, New York, NY, 2013.

[13] R. Kuriakose, C. Anandharamakrishnan, Computational fluid dynamics (CFD) applications in spray drying of food products, Trends in Food Science & Technology 21 (2010) 383–398.

[14] I.C. Kemp, D.E. Oakley, Modelling of particulate drying in theory and practice, Drying Technology 20 (2002) 1699–1750.

[15] T.T.H. Tran, M. Jaskulski, E. Tsotsas, Reduction of a model for single droplet drying and application to CFD of skim milk spray drying, Drying Technology (2017) 1–13.

[16] S.X.Q. Lin, X.D. Chen, D.L. Pearce, Desorption isotherm of milk powders at elevated temperatures and over a wide range of relative humidity, Journal of Food Engineering 68(2005), 257-264.

[17] T.T.H. Tran, J.G. Avila-Acevedo, E. Tsotsas, Enhanced methods for experimental investigation of single droplet drying kinetics and application to lactose/water, Drying Technology 34 (2016) 1185–1195.